Air-liquid interphase culture confers SARS-CoV-2 susceptibility to A549 alveolar epithelial cells

Michihito Sasaki[1]*, Mai Kishimoto[1], Yukari Itakura[1], Koshiro Tabata[1], Kittiya Intaruck[1], Kentaro Uemura[1,2,3], Shinsuke Toba[1,2], Takao Sanaki[1,2], Akihiko Sato[1,2], William W. Hall[4,5,6], Yasuko Orba[1,4] and Hirofumi Sawa[1,4,6,7]

[1]Division of Molecular Pathobiology, International Institute for Zoonosis Control, Hokkaido University, Sapporo, 001-0020, Japan

[2]Shionogi & Co., Ltd., Osaka, 541-0045, Japan

[3]Laboratory of Biomolecular Science, Faculty of Pharmaceutical Science, Hokkaido University, Sapporo, 060-0812, Japan

[4]International Collaboration Unit, International Institute for Zoonosis Control, Hokkaido University, Sapporo, 001-0020, Japan

[5]National Virus Reference Laboratory, University College Dublin, Belfield, Dublin, 4, Ireland

[6]Global Virus Network, Baltimore, Maryland, 21201, USA

[7]One Health Research Center, Hokkaido University, Sapporo, 060-0818, Japan

*Corresponding author:

Michihito Sasaki, E-mail: m-sasaki@czc.hokudai.ac.jp

Abstract

The human lung cell A549 is susceptible to infection with a number of respiratory viruses. However, A549 cells are resistant to Severe Acute Respiratory Syndrome-Coronavirus-2 (SARS-CoV-2) infection in conventional submerged culture, and this would appear to be due to low expression levels of the SARS-CoV-2 entry receptor: angiotensin-converting enzyme-2 (ACE2). Here, we examined SARS-CoV-2 susceptibility to A549 cells after adaptation to air-liquid interface (ALI) culture. A549 cells in ALI culture yielded a layer of mucus on their apical surface, exhibited decreased expression levels of the proliferation marker KI-67 and intriguingly became susceptible to SARS-CoV-2 infection. We found that A549 cells increased the endogenous expression levels of ACE2 and TMPRSS2 following adaptation to ALI culture conditions. Camostat, a TMPRSS2 inhibitor, reduced SARS-CoV-2 infection in ALI-cultured A549 cells. These findings indicate that ALI culture switches the phenotype of A549 cells from resistance to susceptibility to SARS-CoV-2 infection through upregulation of ACE2 and TMPRSS2.

Keywords

SARS-CoV-2; A549 cells; Air-liquid interface; ACE2; TMPRSS2; Viral entry

1. Introduction

Severe Acute Respiratory Syndrome-Coronavirus-2 (SARS-CoV-2) causes severe respiratory diseases in humans. The virus spike (S) protein is a glycoprotein localized on SARS-CoV-2 virion surface and triggers viral entry and membrane fusion in target cells through the interaction with host factors: entry receptors and proteases [1]. To date, two type I transmembrane proteins have been identified as entry receptors for SARS-CoV-2: angiotensin-converting enzyme-2 (ACE2) and neuropilin-1 (NRP1) [2-4]. In particular, the interaction between ACE2 and S protein has attracted attention, because emerging SARS-CoV-2 variants possess amino acid substitutions in the receptor binding domain of S protein which can increase the binding affinity to human ACE2 [5]. In addition, the exogenous expression of ACE2 confers SARS-CoV-2 susceptibility to cells which are normally resistant to infection [6,7]; therefore, ACE2 is a major determinant of SARS-CoV-2 susceptibility. On the other hand, certain host proteases proteolytically activate (or prime) S protein for membrane fusion. For example, TMPRSS2 is a host serine protease which act as a priming enzyme of SARS-CoV-2 S protein. TMPRSS2 mediates direct fusion of SARS-CoV-2 virion on the plasma membrane and facilitates SARS-CoV-2 entry [2,8]. Collectively, cells expressing both ACE2 and TMPRSS2 are highly permissive to SARS-CoV-2 entry.

Airway epithelial cells are positive for ACE2/TMPRSS2 and are primary targets of *in vivo* infection of SARS-CoV-2 [9,10]. Primary human airway epithelial cells can be cultured and used for basic research studies and antiviral development [11-13]. In experiments, primary airway epithelial cells are differentiated and maintained under an air-

liquid interface under (ALI) culture condition, which allows cells to grow on microporous membranes in culture inserts with air exposure and culture medium through the basolateral side. It has been reported that 96% of expressed genes represent similar expression patterns between brushed biopsy of nasal epithelial cells and those cultured under ALI conditions [14]. In comparison with conventional submerged culture condition where cells are grown on a plastic surface with overlayed culture medium, primary airway epithelial cells in ALI culture recapitulate the transcriptional profile of *in vivo* airway epithelia [15]. The ALI culture method is a more physiologically relevant way for infection of primary airway epithelial cells and provides an appropriate *ex vivo* respiratory model.

A549 and Calu-3 cells are human lung-derived epithelial cells and widely used for studies of virus infection. In contrast to Calu-3 cells, only limited entry and growth of SARS-CoV-2 occurs in A549 cells [7]. The decreased susceptibility of A549 cells to SARS-CoV-2 infection was attributed to the low expression level of ACE2 and the retinoic acid-inducible gene-I (RIG-I)-mediated antiviral response [1,16]. These studies were performed by inoculation of SARS-CoV-2 to cells under submerged culture conditions. In contrast, these cell lines can be cultured and differentiated under ALI conditions. ALI-cultured A549 cells are used for cell-based toxicity assays by inhalation exposure of exhausts, nanoparticles and chemical compounds [17-19]. A549 cells exert different expression profiles of genes involved in cellular processes such as those in the cell cycle, DNA damage repair and transporters between in submerged and ALI cultures [20,21]. In the present study, we compared the susceptibility of A549 cells to SARS-CoV-2 infection under these culture conditions.

2. Materials and Methods

2.1. Cells

Calu-3 cells (ATCC, Manassas, VA) were maintained in Eagle's Minimum Essential Medium (MEM) supplemented with 10% fetal bovine serum (FBS). A549 (RIKEN BRC, Tsukuba, Japan) and Vero-TMPRSS2 [22] cells were maintained in Dulbecco's Modified Eagle's Medium (DMEM) supplemented with 10% FBS. All cells were incubated at 37°C with 5% CO_2. Generation of human ACE2- and TMPRSS2-expressing cells were described previously [22]. A549 cells stably expressing ACE2 and TMPRSS2 were selected in the presence of puromycin (for ACE2) or blasticidin S (for TMPRSS2).

2.2. Viruses

SARS-CoV-2 WK-521 strain (EPI_ISL_408667) were provided by Dr. Saijyo and Dr. Shimojima (National Institute of Infectious Diseases, Tokyo, Japan). The original stock was prepared by inoculation of Vero-TMPRSS2 cells and titrated by plaque assay as previously described [22].

2.3. Immunoblotting

Cells were lysed in lysis buffer (1% NP-40; 20 mM Tris-HCl, pH 7.5; 150 mM NaCl; and 5 mM EDTA) supplemented with cOmplete ULTRA protease inhibitor cocktail (Roche Diagnostics, Indianapolis, IN). Cell lysate was analyzed by SDS-PAGE and immunoblotting using anti-ACE2 (4355T, Cell Signaling Technology, Danvers, MA) or

anti-TMPRSS2 (ab92323, Abcam, Cambridge, UK) antibodies. HRP-conjugated anti-β-actin antibody (PM053-7, MBL, Tokyo, Japan) was used to detect the loading control. Immune complexes were detected using HRP-conjugated anti-rabbit IgG secondary antibody and the Immobilon Western Chemiluminescent HRP Substrate (Millipore; Merck, Darmstadt, Germany).

2.4. A549 cell culture in the air-liquid interface (ALI)

Millicell culture inserts for 24-well plate with a 0.4 μm pore size polyethylene terephthalate (PET) membrane and 0.3 cm^2 culture area (Millipore; Merck) were coated with type I collagen. A549 cells were seeded onto the insert at 100,000 cells and cultured in DMEM supplemented with 10% FBS for 24 h. Culture medium in the apical and basal chambers were then replaced with PneumaCult ALI medium (STEMCELL Technologies, Vancouver, Canada). On day 3 after seeding, the cells were subjected to air-lift by removing medium from both the apical and basal chambers but supplying fresh PneumaCult ALI medium only in the basal chamber. Cells were maintained in ALI for at least an additional 21 days. The culture medium in the basal chamber was changed every 3 days and the apical area was washed with the culture medium every 7 days.

2.5. Cell staining

A549 cells in the culture insert were fixed with 10% phosphate-buffered formalin before ALI culture or after ALI culture for 21 days. Clipped cells with PET membranes were embedded in paraffin, sectioned at 4 μm-thickness and mounted on Platinum PRO micro

128 slide glass (Matsunami Glass, Osaka, Japan). Slides were stained with hematoxylin and
129 eosin (H&E) and periodic acid-schiff (PAS) staining (MUTO Pure Chemicals, Tokyo,
130 Japan).
131
132 **2.6. Multi-cycle growth of SARS-CoV-2**
133 For assays in submerged culture, cells in 24-well plates were inoculated with SARS-CoV-2
134 at a multiplicity of infection (MOI) of 1 (Fig. 1A), 10 (Fig. 1A-1C) or 0.1 (Fig. 1G and 1H)
135 for 1 h. Cells were then washed with PBS to remove unabsorbed viruses and cultured in
136 fresh medium with 2% FBS. The culture supernatants for virus titration were harvested at
137 the indicated time points. For assays in ALI culture, ALI-cultured A549 cells were infected
138 at the apical surface with SARS-CoV-2 at 50,000 plaque forming unit (pfu) in 100 μl of
139 culture medium. After 1 h of incubation, the apical area of cells was washed twice with
140 PBS, and then cells were maintained under ALI culture conditions. At the indicated time
141 points, the mucus fluids containing progeny viruses in the apical area were suspended by
142 incubation with 200 μl of culture medium for 30 min. The harvested fluids were subjected
143 to virus titration.
144
145 **2.7. Quantitative reverse-transcription PCR (qRT-PCR)**
146 Total RNA was extracted from cells with TRIzol (Invitrogen; Themo Fisher Scientific,
147 Waltham, MA) and Direct-zol RNA MiniPrep kit (Zymo Research, Irvine, CA). The RNA
148 samples were analyzed by qRT-PCR with Thunderbird Probe One-step Probe qRT-PCR Kit
149 (Toyobo, Osaka, Japan). Probe and primers targeting SARS-CoV-2 nucleocapsid (N) gene

were used for viral RNA quantification and described previously as N2 set [23]. The following Taqman Gene Expression Assays (Applied Biosystems; Thermo Fisher Scientific) consisting of predesigned probe and primers were used for host gene expression analysis: KI-67 (Hs01032443_m1), ACE2 (Hs01085333_m1), NRP1 (Hs00826128_m1), Cathepsin L (Hs00964650_m1), TMPRSS2 (Hs00237175_m1) and β-actin (Hs99999903_m1). Negative samples were included in the analysis with Ct values set at the limit of detection value (Ct=50). RNA levels were normalized to β-actin and calculated by the ΔΔCt method.

2.8. Virus infection assay with the TMPRSS2 inhibitor, camostat mesylate.

ALI-cultured A549 cells were infected at the apical surface with SARS-CoV-2 at 250,000 pfu in the presence of 50 μM camostat mesylate (FUJIFILM Wako Pure chemical, Osaka, Japan) for 2 h. The apical area of cells was washed three times with PBS and then cells were maintained under ALI culture for 4 h. At 6 h post-infection (hpi), cells were mixed with TRIzol reagent and subjected to RNA extraction and qRT-PCR assay as described above.

3. Results

3.1. The susceptibility of A549 cells to SARS-CoV-2 infection

A549 and Calu-3 cells were cultured in conventional submerged condition and inoculated with SARS-CoV-2 at different MOIs. The infectious virus titers and virus RNA levels were increased in Calu-3 cells infected with SARS-CoV-2 in a time-dependent

172 manner (Fig. 1A and 1B). In contrast, SARS-CoV-2 replication was barely detectable in
173 A549 cells even at a high MOI using virus titration and qRT-PCR assays (Fig. 1A and 1C).
174 It has been reported that exogenous expression of ACE2 renders A549 cells susceptible to
175 SARS-CoV-2 infection [24-26]. We also generated A549 cells with overexpression of
176 ACE2 and/or TMPRSS2 (A549-A2, -T2 and -A2T2 cells). The enhanced expression of the
177 transduced genes was validated by qRT-PCR and immunoblotting (Fig. 1D-1F).
178 Immunoblotting analysis revealed that the full-length of ACE2 protein was present in the
179 lysate of A549-A2 but not in that of A549-A2T2 (Fig. 1F), consistent with a previous
180 report that ACE2 is processed by TMPRSS2 but maintains its receptor activity for SARS-
181 CoV [27]. SARS-CoV-2 replication was observed exclusively in ACE2-overexpressing
182 A549 cells (A549-A2 and A549-A2T2 cells) (Fig. 1G and 1H). The virus titers in A549-
183 A2T2 cells were higher than those in A549-A2 at 24 and 48 hpi (Fig. 1G), indicating that
184 TMPRSS2 facilitates SARS-CoV-2 infection in the presence of ACE2 in A549 cells.
185
186 **3.2. The susceptibility of A549 cells under ALI-culture to SARS-CoV-2 infection**
187 Primary human nasal and bronchial epithelial cells can be differentiated under ALI
188 culture conditions. The differentiated epithelial cells are susceptible to SARS-CoV-2
189 infection and used as an *ex vivo* model to study SARS-CoV-2 infection in the human
190 airway [11-13]. We examined the impact of ALI culture on the susceptibility of A549 cells
191 to SARS-CoV-2 infection. A549 cells were seeded onto culture inserts and fed commercial
192 differentiation medium only in the basal chamber for ALI culture (Fig. 2A). A549 cells
193 formed a monolayer in the insert under submerged culture with maintenance medium of

194 DMEM containing 10% FBS (non-ALI), while the cells increased in number with a
195 multilayered structure in ALI culture (Fig. 2B). A549 cells in ALI culture yielded a layer of
196 mucus which was synthesized by the cells and detected by PAS staining (Fig. 2C). The
197 expression levels of the proliferation marker KI-67 was markedly decreased in A549 cells
198 in ALI culture (Fig. 2D) as previously reported [18]. SARS-CoV-2 was inoculated onto the
199 apical surface of A549 cells adapted to ALI culture (ALI day 21). A549 cells under
200 submerged culture (non-ALI) was used as a control. Viral replication and progeny viruses
201 were observed only in A549 cells under ALI conditions (Fig. 2E and 2F), indicating that
202 ALI culture confers susceptibility of SARS-CoV-2 to infection of A549 cells.
203
204 **3.3 Upregulated expression of ACE2 and TMPRSS2 in A549 cells in ALI-culture**
205 ALI-culture reportedly upregulates the expression of ACE2 in primary human
206 tracheobronchial epithelial cells [28]. Therefore, we compared the expression levels of
207 ACE2 between A549 cells in submerged non-ALI and ALI cultures. After 21 days of ALI
208 culture, the ACE2 level was markedly elevated more than 200-fold above non-ALI culture
209 (Fig. 3A). In contrast, a consistent expression level of another SARS-CoV-2 entry receptor,
210 NRP1, was observed in A549 cells through the culture period (from day 0 to day 21, Fig.
211 3B). We also examined the expression levels of host proteases, cathepsin and TMPRSS2,
212 which are responsible for SARS-CoV-2 S protein priming in membrane fusion. The
213 increased expression of both proteases was observed in ALI-cultured A549 cells (Fig. 3C
214 and 3D). Notably, TMPRSS2 expression levels were more than three orders of magnitude
215 higher after 21 days of ALI culture (Fig. 3D). In order to investigate the impact of increased

expression of TMPRSS2 on SARS-CoV-2 entry, we examined the inhibitory effect of camostat, a TMPRSS2 inhibitor, on SARS-CoV-2 entry into the cells. Camostat inhibited viral entry into ALI-cultured A549 cells (Fig. 3E), indicating that TMPRSS2 facilitates SARS-CoV-2 entry in ALI-cultured A549 cells.

4. Discussion

ALI culture conditions allow the differentiation of primary airway epithelial cells under the similar condition as the physiological state. Human lung-derived cells A549 and Calu-3 can also be differentiated under ALI culture and are used as models for toxicological and pharmacological studies with exhausts, nanoparticles and chemical compounds [17-19]. Here, we applied ALI-cultured A549 cells for experiments with SARS-CoV-2. In contrast to A549 cells in submerged culture, A549 cells in ALI-culture permitted SARS-CoV-2 infection and yielded sufficient level of progeny virus without exogenous gene expression. These results indicated that ALI-culture switches the phenotype of A549 cells from resistance to susceptibility to SARS-CoV-2 infection.

A549 is a human lung carcinoma-derived cell line and widely used in virological studies. This cell line showed limited endogenous ACE2 expression level and was non-permissive to SARS-CoV-2 infection under submerged culture conditions (Fig. 1F-1H) [7]. Our study and other studies demonstrated that exogenous expression of human ACE2 mediates SARS-CoV-2 entry and renders A549 cells permissive for SARS-CoV-2 infection [24-26]. Upregulation of endogenous ACE2 level is the possible primary cause of the susceptibility of ALI-cultured A549 cells to SARS-CoV-2 infection. ALI culture also

238 increased the expression level of TMPRSS2 in A549 cells, which activates the S protein
239 and facilitates cellular entry of SARS-CoV-2. Since camostat, a TMPRSS2 inhibitor,
240 reduced SARS-CoV-2 entry into ALI-cultured A549 cells, TMPRSS2 plays a role in
241 SARS-CoV-2 infection in the cells.
242 One limitation of our study is that we could not infer the mechanism of ACE2 and
243 TMPRSS2 upregulations under ALI culture conditions. In contrast to ACE2 and
244 TMPRSS2, the level of another SARS-CoV-2 receptor NRP1 was consistent between cells
245 in submerged- and ALI-culture. ACE2 expression is reportedly upregulated by ALI culture
246 in primary human tracheobronchial epithelial cells [28]. These findings indicate that ALI
247 culture increases the expression levels of specific host factors involved in SARS-CoV-2
248 infection and this event is not specific for the A549 cell line. Qiao *et al*. have currently
249 proposed that the androgen receptor enhances expression levels of both ACE2 and
250 TMPRSS2 in lung epithelial cells through the binding to their promoter regions [29].
251 Investigation of the relationship between androgen receptor and ACE2/TMPRSS2
252 expression event in A549 cells may provide insights into the mechanism of ACE2 and
253 TMPRSS2 upregulations in ALI culture.
254 In conclusion, this study demonstrated that ALI culture confers SARS-CoV-2
255 susceptibility to A549 cells. Unlike primary human airway cells, ALI-cultured A549 cells
256 are free from donor variation and established easily. ALI-cultured A549 cells thus could be
257 used as an alternative model to primary human airway cells for investigation of the inhaled
258 exposure of SARS-CoV-2 and the evaluation of antivirals against SARS-CoV-2.
259

Acknowledgments

We thank Drs. Saijyo, Shimojima and Ito at National Institute of Infectious Diseases, Japan for providing SARS-CoV-2 WK-521 strain. This work was supported by the Japan Agency for Medical Research and Development (AMED) (PJ21fk0108104, JP21wm0125008, PJ20fk0108509), Japan Science and Technology Agency (JST) Moonshot R&D under Grant numbers JPMJMS2025, the World-leading Innovative and Smart Education (WISE) Program (1801) from the Ministry of Education, Culture, Sports, Science, and Technology, Japan, and the fund from the Atlantic Philanthropies director.

Declaration of competing interest

The authors K.U., S.T., T.S., and A.S. are employees of Shionogi & Co., Ltd. Other authors declare no competing interests.

References

[1] N. Murgolo, A.G. Therien, B. Howell, D. Klein, et al., SARS-CoV-2 tropism, entry, replication, and propagation: Considerations for drug discovery and development, PLoS Pathog 17 (2021) e1009225. 10.1371/journal.ppat.1009225.

[2] M. Hoffmann, H. Kleine-Weber, S. Schroeder, N. Krüger, et al., SARS-CoV-2 Cell Entry Depends on ACE2 and TMPRSS2 and Is Blocked by a Clinically Proven Protease Inhibitor, Cell 181 (2020) 271-280.e278. 10.1016/j.cell.2020.02.052.

[3] L. Cantuti-Castelvetri, R. Ojha, L.D. Pedro, M. Djannatian, et al., Neuropilin-1 facilitates SARS-CoV-2 cell entry and infectivity, Science (2020). 10.1126/science.abd2985.

[4] J.L. Daly, B. Simonetti, K. Klein, K.E. Chen, et al., Neuropilin-1 is a host factor for SARS-CoV-2 infection, Science (2020). 10.1126/science.abd3072.

[5] T.P. Peacock, R. Penrice-Randal, J.A. Hiscox, W.S. Barclay, SARS-CoV-2 one year on: evidence for ongoing viral adaptation, J Gen Virol 102 (2021). 10.1099/jgv.0.001584.

[6] K. Uemura, M. Sasaki, T. Sanaki, S. Toba, Y. et al., MRC5 cells engineered to express ACE2 serve as a model system for the discovery of antivirals targeting SARS-CoV-2, Sci Rep 11 (2021) 5376. 10.1038/s41598-021-84882-7.

[7] E. Saccon, X. Chen, F. Mikaeloff, J.E. Rodriguez, et al., Cell-type-resolved quantitative proteomics map of interferon response against SARS-CoV-2, iScience 24 (2021) 102420. 10.1016/j.isci.2021.102420.

[8] S. Matsuyama, N. Nao, K. Shirato, M. Kawase, et al., Enhanced isolation of SARS-CoV-2 by TMPRSS2-expressing cells, Proc Natl Acad Sci U S A 117 (2020) 7001-7003. 10.1073/pnas.2002589117.

[9] C. Muus, M.D. Luecken, G. Eraslan, L. Sikkema, et al., Single-cell meta-analysis of

296 SARS-CoV-2 entry genes across tissues and demographics, Nat Med 27 (2021) 546-559.
297 10.1038/s41591-020-01227-z.
298 [10] A.F. Rendeiro, H. Ravichandran, Y. Bram, V. Chandar, et al., The spatial landscape of
299 lung pathology during COVID-19 progression, Nature 593 (2021) 564-569. 10.1038/s41586-
300 021-03475-6.
301 [11] S. Hao, K. Ning, C.A. Kuz, K. Vorhies, et al., Long-Term Modeling of SARS-CoV-2
302 Infection of In Vitro Cultured Polarized Human Airway Epithelium, mBio 11 (2020).
303 10.1128/mBio.02852-20.
304 [12] A. Pizzorno, B. Padey, T. Julien, S. Trouillet-Assant, et al., Characterization and
305 Treatment of SARS-CoV-2 in Nasal and Bronchial Human Airway Epithelia, Cell Rep Med
306 1 (2020) 100059. 10.1016/j.xcrm.2020.100059.
307 [13] V.K. Outlaw, F.T. Bovier, M.C. Mears, M.N. Cajimat, et al., Inhibition of Coronavirus
308 Entry In Vitro and Ex Vivo by a Lipid-Conjugated Peptide Derived from the SARS-CoV-2
309 Spike Glycoprotein HRC Domain, mBio 11 (2020). 10.1128/mBio.01935-20.
310 [14] B. Ghosh, B. Park, D. Bhowmik, K. Nishida, et al., Strong correlation between air-liquid
311 interface cultures and in vivo transcriptomics of nasal brush biopsy, Am J Physiol Lung Cell
312 Mol Physiol 318 (2020) L1056-L1062. 10.1152/ajplung.00050.2020.
313 [15] A.A. Pezzulo, T.D. Starner, T.E. Scheetz, G.L. Traver, et al., The air-liquid interface and
314 use of primary cell cultures are important to recapitulate the transcriptional profile of in vivo
315 airway epithelia, Am J Physiol Lung Cell Mol Physiol 300 (2011) L25-31.
316 10.1152/ajplung.00256.2010.
317 [16] T. Yamada, S. Sato, Y. Sotoyama, Y. Orba, et al., RIG-I triggers a signaling-abortive anti-
318 SARS-CoV-2 defense in human lung cells, Nat Immunol (2021). 10.1038/s41590-021-
319 00942-0.

[17] C. Barraud, C. Corbière, I. Pottier, E. Estace, et al., Impact of after-treatment devices and biofuels on diesel exhausts genotoxicity in A549 cells exposed at air-liquid interface, Toxicol In Vitro 45 (2017) 426-433. 10.1016/j.tiv.2017.04.025.

[18] D. Movia, D. Bazou, Y. Volkov, A. Prina-Mello, Multilayered Cultures of NSCLC cells grown at the Air-Liquid Interface allow the efficacy testing of inhaled anti-cancer drugs, Sci Rep 8 (2018) 12920. 10.1038/s41598-018-31332-6.

[19] R.W. He, M.E. Gerlofs-Nijland, J. Boere, P. Fokkens, et al., Comparative toxicity of ultrafine particles around a major airport in human bronchial epithelial (Calu-3) cell model at the air-liquid interface, Toxicol In Vitro 68 (2020) 104950. 10.1016/j.tiv.2020.104950.

[20] K. Öhlinger, T. Kolesnik, C. Meindl, B. Gallé, et al., Air-liquid interface culture changes surface properties of A549 cells, Toxicol In Vitro 60 (2019) 369-382. 10.1016/j.tiv.2019.06.014.

[21] J. Wu, Y. Wang, G. Liu, Y. Jia, et al., Characterization of air-liquid interface culture of A549 alveolar epithelial cells, Braz J Med Biol Res 51 (2017) e6950. 10.1590/1414-431X20176950.

[22] M. Sasaki, K. Uemura, A. Sato, S. Toba, et al., SARS-CoV-2 variants with mutations at the S1/S2 cleavage site are generated in vitro during propagation in TMPRSS2-deficient cells, PLoS Pathog 17 (2021) e1009233. 10.1371/journal.ppat.1009233.

[23] K. Shirato, N. Nao, H. Katano, I. Takayama, et al., Development of Genetic Diagnostic Methods for Detection for Novel Coronavirus 2019(nCoV-2019) in Japan, Jpn J Infect Dis 73 (2020) 304-307. 10.7883/yoken.JJID.2020.061.

[24] D. Blanco-Melo, B.E. Nilsson-Payant, W.C. Liu, S. Uhl, et al., Imbalanced Host Response to SARS-CoV-2 Drives Development of COVID-19, Cell 181 (2020) 1036-1045.e1039. 10.1016/j.cell.2020.04.026.

[25] M. de Vries, A.S. Mohamed, R.A. Prescott, A.M. Valero-Jimenez, et al., A comparative analysis of SARS-CoV-2 antivirals characterizes 3CL^{pro} inhibitor PF-00835231 as a potential new treatment for COVID-19., J Virol (2021). 10.1128/JVI.01819-20.

[26] Y. Liu, G. Hu, Y. Wang, W. Ren, et al., Functional and genetic analysis of viral receptor ACE2 orthologs reveals a broad potential host range of SARS-CoV-2, Proc Natl Acad Sci U S A 118 (2021). 10.1073/pnas.2025373118.

[27] A. Heurich, H. Hofmann-Winkler, S. Gierer, T. Liepold, et al., TMPRSS2 and ADAM17 cleave ACE2 differentially and only proteolysis by TMPRSS2 augments entry driven by the severe acute respiratory syndrome coronavirus spike protein, J Virol 88 (2014) 1293-1307. 10.1128/JVI.02202-13.

[28] H.P. Jia, D.C. Look, L. Shi, M. Hickey, et al., ACE2 receptor expression and severe acute respiratory syndrome coronavirus infection depend on differentiation of human airway epithelia, J Virol 79 (2005) 14614-14621. 10.1128/JVI.79.23.14614-14621.2005.

[29] Y. Qiao, X.M. Wang, R. Mannan, S. Pitchiaya, et al., Targeting transcriptional regulation of SARS-CoV-2 entry factors, Proc Natl Acad Sci U S A (2020). 10.1073/pnas.2021450118.

Figure Legends

Fig. 1. Infectivity of SARS-CoV-2 in A549 cells under submerged culture condition

(A) Growth curves of SARS-CoV-2 in A549 and Calu-3 cells. Viral titers in the culture supernatant were determined using a plaque assay. (B and C) SARS-CoV-2 RNA levels in Calu-3 cells (B) and A549 cells (C) were quantified by qRT-PCR and were normalized to the expression levels of β-actin. (D and E) Expression levels of exogenously transduced ACE2 (D) and TMPRSS2 (E) were quantified by qRT-PCR and normalized to the expression levels of β-actin. (F) Expression of exogenously transduced proteins was detected by Western Blotting with antibodies specific to the proteins indicated on the left. The full-length and cleaved forms of TMPRSS2 are indicated by close and open arrowheads, respectively. Asterisks indicate nonspecific bands that cross-reacted with anti-TMPRSS2 antibody. (G) Growth curves of SARS-CoV-2 in A549 cells expressing ACE2 and TMPRSS2. Viral titers in the culture supernatant were determined using a plaque assay. (H) The levels of SARS-CoV-2 N gene at 72 hpi were quantified by qRT-PCR and normalized to the expression levels of β-actin. The values in the graphs are expressed as the mean ± SD of triplicate samples.

Fig. 2. Infectivity of SARS-CoV-2 in A549 cells under air-liquid interface culture condition

(A) Schematic representation of the ALI culture system. A549 cells were seeded onto a culture insert with growth medium (non-ALI condition). The medium at the apical chamber was then removed to start the ALI culture (ALI day 0). Cells were maintained for another

21 days by supplying ALI medium to the basal chamber (ALI day 21). (B and C) A549 cells in non-ALI and ALI day 21 were examined by hematoxylin and eosin (H&E) (B) and periodic acid-schiff (PAS) staining (C). Mucus in cells displayed purple color after PAS staining. Scale bars = 100 μm. (D and E) Relative levels of KI-67 (D) and SARS-CoV-2 N (E) were measured by qRT-PCR and normalized to the expression levels of β-actin. (F) Growth curves of SARS-CoV-2 in A549 cells in non-ALI and ALI culture conditions. The mucus fluids in the apical area were suspended in culture medium and subjected to viral titration using a plaque assay. The values in the graphs are expressed as the mean ± SD of triplicate samples. * $p < 0.05$, *** $p < 0.001$, two-tailed Student's *t*-test.

Fig. 3. Gene expression levels of host factors involved in SARS-CoV-2 entry

(A-D) Relative expression levels of ACE2 (A), NRP1 (B), cathepsin L (C) and TMPRSS2 (D) in A549 cells during the adaptation to ALI culture were measured by qRT-PCR. β-actin mRNA levels were used as the reference control. (E) ALI-cultured A549 cells were infected with SARS-CoV-2 in the presence of 50 μM camostat. Viral RNA levels at 6 hpi were measured by qRT-PCR and normalized to the expression levels of β-actin. The values in the graphs are expressed as the mean ± SD of triplicate samples. ** $p < 0.01$, two-tailed Student's *t*-test.

Figure 1

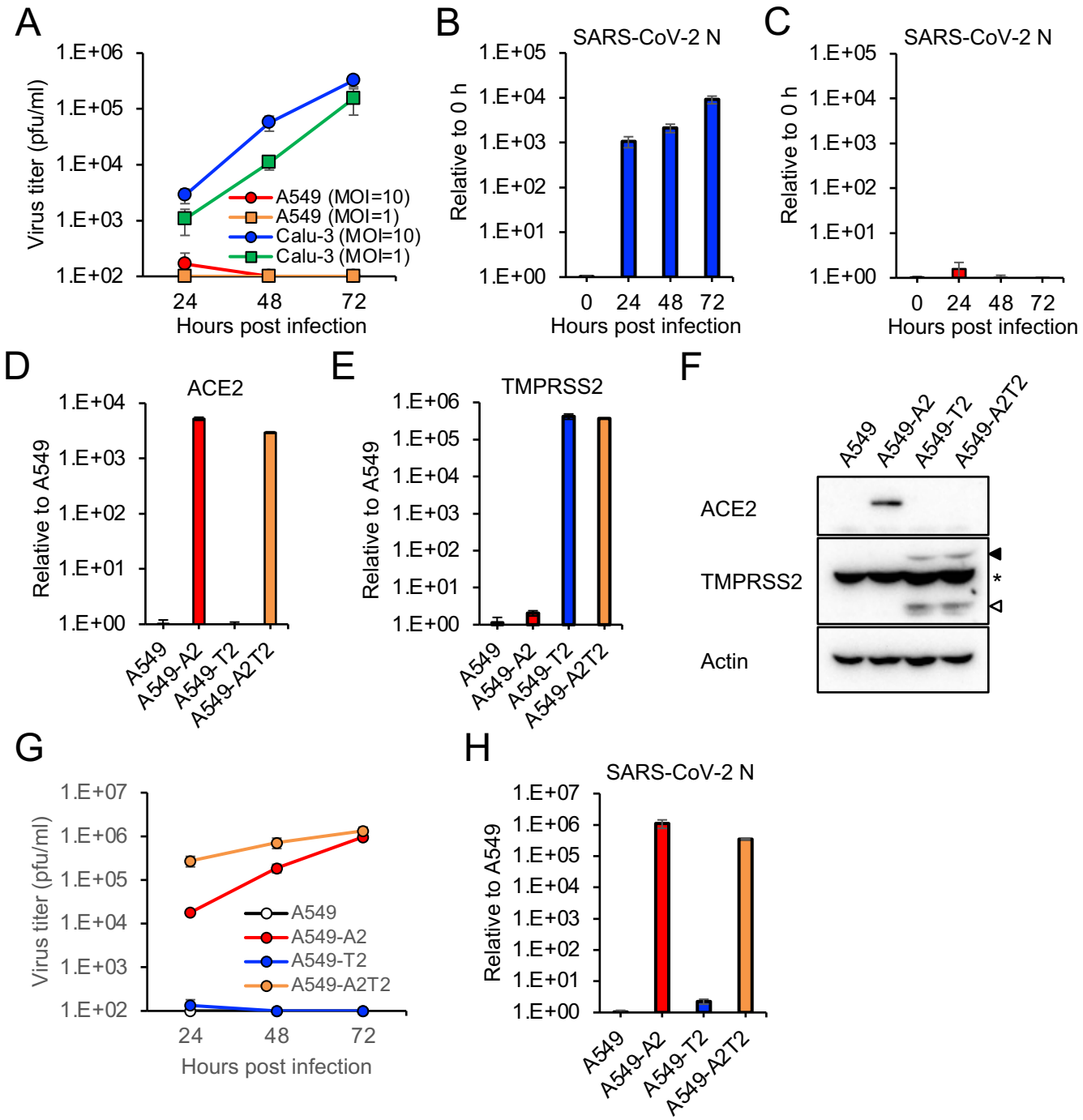
A
Virus titer (pfu/ml)
1.E+06
1.E+05
1.E+04
1.E+03
1.E+02
24
48
72
Hours post infection
A549 (MOI=10)
A549 (MOI=1)
Calu-3 (MOI=10)
Calu-3 (MOI=1)
B
SARS-CoV-2 N
Relative to 0 h
1.E+05
1.E+04
1.E+03
1.E+02
1.E+01
1.E+00
0
24
48
72
Hours post infection
C
SARS-CoV-2 N
Relative to 0 h
1.E+05
1.E+04
1.E+03
1.E+02
1.E+01
1.E+00
0
24
48
72
Hours post infection
D
ACE2
Relative to A549
1.E+04
1.E+03
1.E+02
1.E+01
1.E+00
A549
A549-A2
A549-T2
A549-A2T2
E
TMPRSS2
Relative to A549
1.E+06
1.E+05
1.E+04
1.E+03
1.E+02
1.E+01
1.E+00
A549
A549-A2
A549-T2
A549-A2T2
F
A549
A549-A2
A549-T2
A549-A2T2
ACE2
TMPRSS2
Actin
*
G
Virus titer (pfu/ml)
1.E+07
1.E+06
1.E+05
1.E+04
1.E+03
1.E+02
24
48
72
Hours post infection
A549
A549-A2
A549-T2
A549-A2T2
H
SARS-CoV-2 N
Relative to A549
1.E+07
1.E+06
1.E+05
1.E+04
1.E+03
1.E+02
1.E+01
1.E+00
A549
A549-A2
A549-T2
A549-A2T2

Figure 2

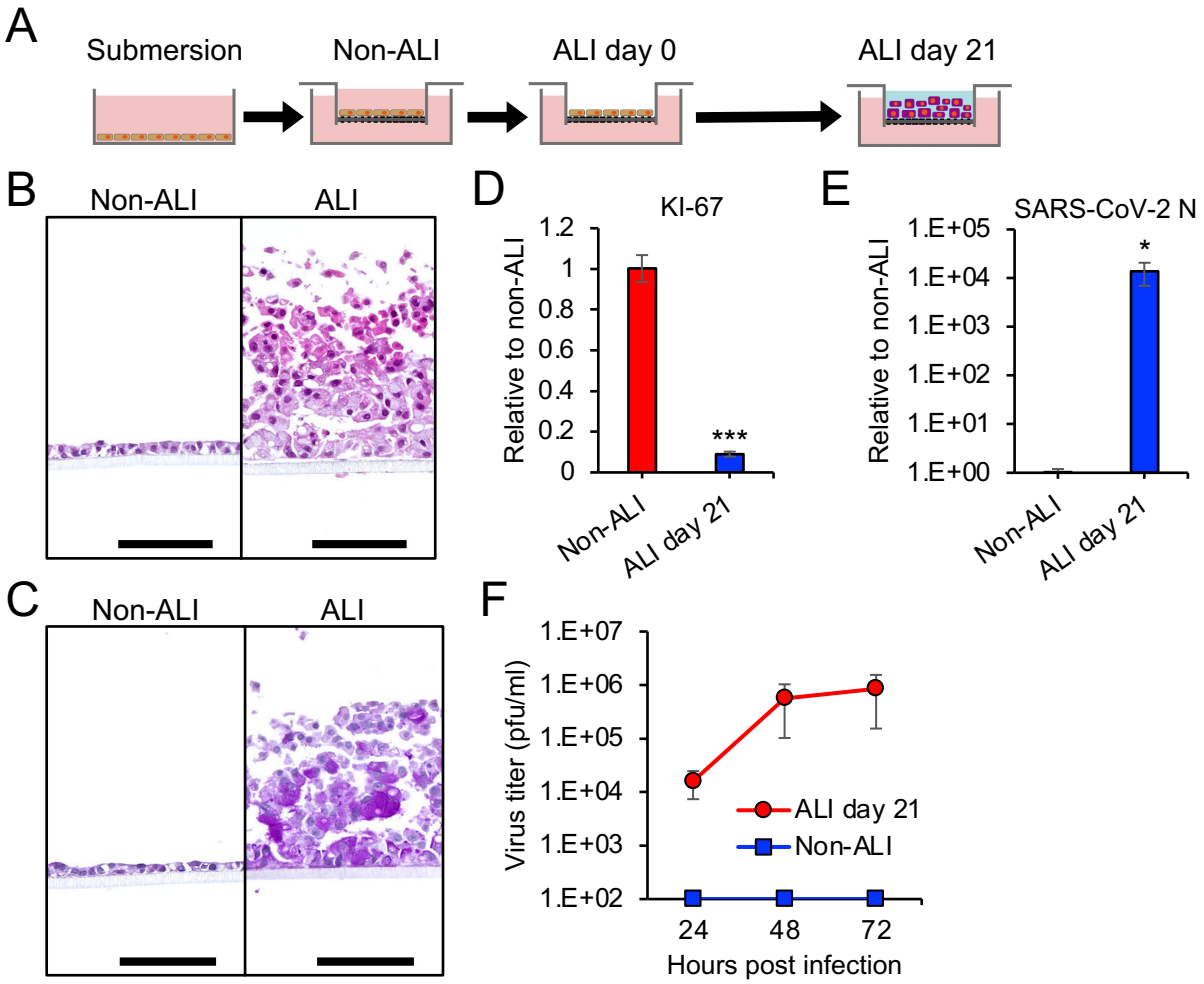
A
Submersion
Non-ALI
ALI day 0
ALI day 21
B
Non-ALI
ALI
C
Non-ALI
ALI
D
KI-67
Relative to non-ALI
1.2
1
0.8
0.6
0.4
0.2
0
***
Non-ALI
ALI day 21
E
SARS-CoV-2 N
Relative to non-ALI
1.E+05
1.E+04
1.E+03
1.E+02
1.E+01
1.E+00
*
Non-ALI
ALI day 21
F
Virus titer (pfu/ml)
1.E+07
1.E+06
1.E+05
1.E+04
1.E+03
1.E+02
ALI day 21
Non-ALI
24
48
72
Hours post infection

Figure 3

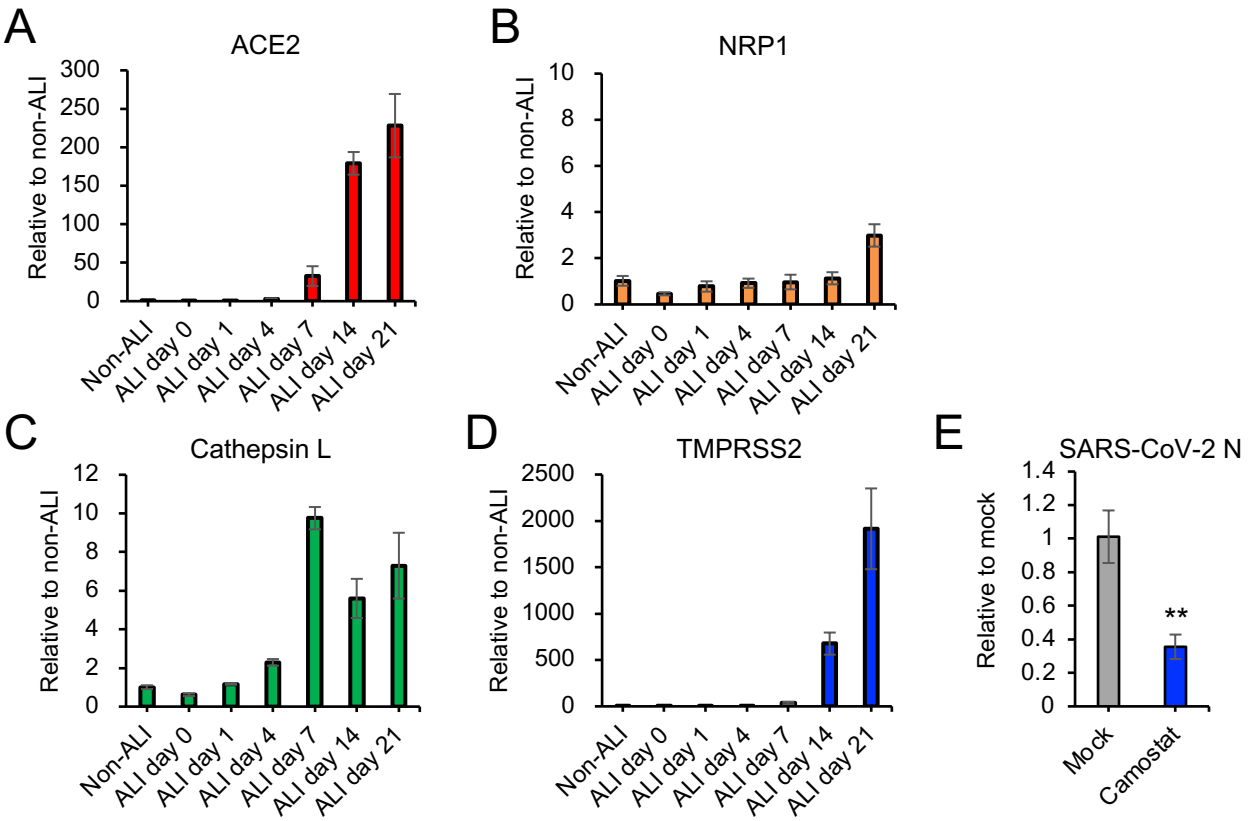
A
ACE2
Relative to non-ALI
300
250
200
150
100
50
0
Non-ALI
ALI day 0
ALI day 1
ALI day 4
ALI day 7
ALI day 14
ALI day 21
B
NRP1
Relative to non-ALI
10
8
6
4
2
0
C
Cathepsin L
Relative to non-ALI
12
10
8
6
4
2
0
D
TMPRSS2
Relative to non-ALI
2500
2000
1500
1000
500
0
E
SARS-CoV-2 N
Relative to mock
1.4
1.2
1
0.8
0.6
0.4
0.2
0
**
Mock
Camostat